Supplementary Information for

A moisture-enabled fully printable power source inspired by electric eels

Lu Yang, Feiyao Yang, Xu Liu, Ke Li, Yaning Zhou, Yangjian Wang, Tianhao Yu, Mengjuan Zhong, Xiaobing Xu, Lijuan Zhang, Wei Shen, and Di Wei
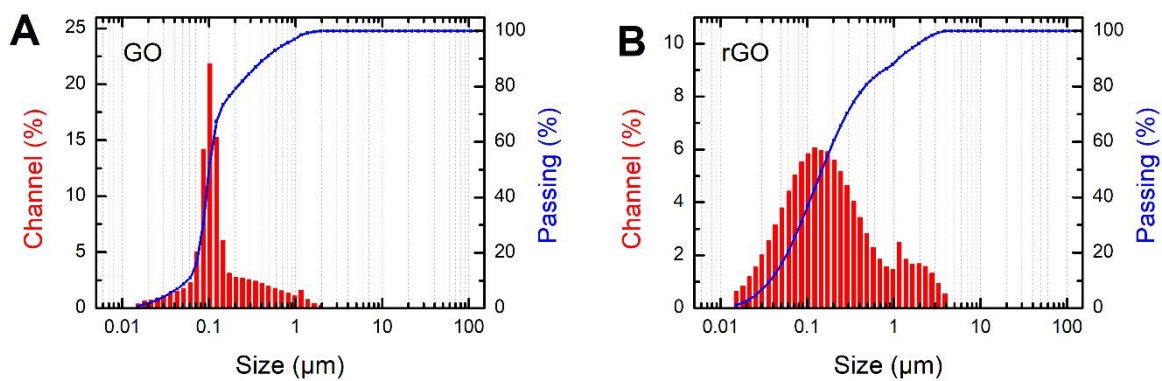
Di Wei
Email: weidi-cnc@pku.edu.cn

This PDF file includes:

> Figures S1 to S9
> Legends for Movies S1 to S2

Other supplementary materials for this manuscript include the following:
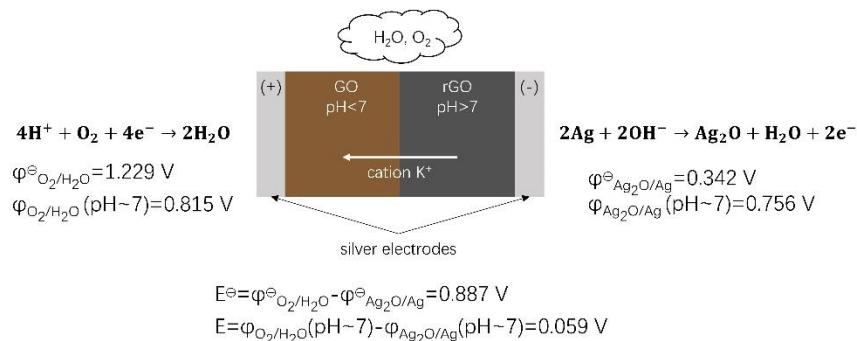
> Movies S1 to S2

Fig. S1. Particle size analysis results of GO and rGO solutions. (*A*) Size distribution of GO solutions dispersed by ultrasonic homogenizer. (*B*) Size distribution of rGO solutions by adding KOH to GO dispersed solutions.
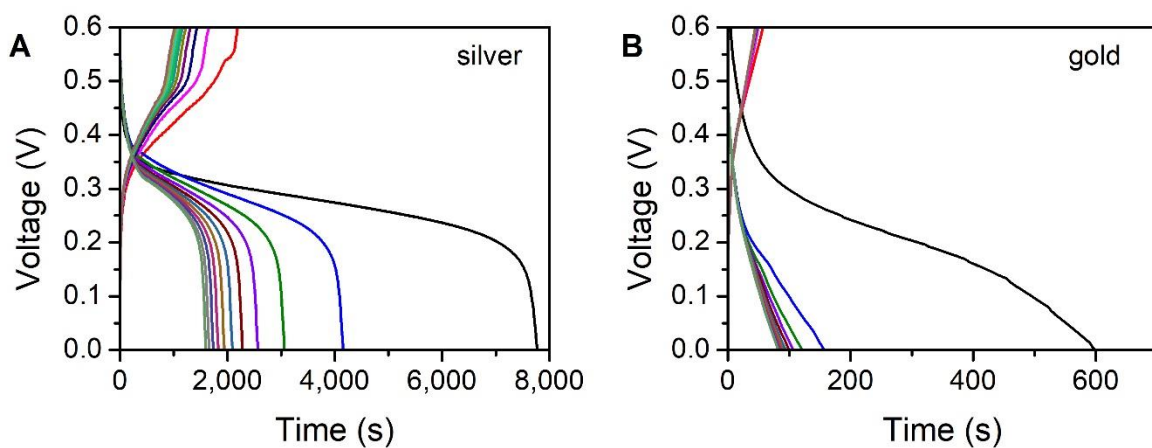
Fig. S2. The galvanostatic charge-discharge cycle performance of drop-casted cells with different electrodes at 0.1 µA (25 °C RH 70%). (*A*) The cycling performance of cell with silver electrodes. The capacity gradually decreases within 10 cycles. (*B*) The cycling performance of cell with gold current collectors. The capacity is much lower than that of cells with silver electrodes and the capacity doesn't change much after initial discharge.

$$4H^+ + O_2 + 4e^- \rightarrow 2H_2O$$

H_2O, O_2

(+) GO pH<7 | rGO pH>7 (−)

cation K$^+$

silver electrodes

$$2Ag + 2OH^- \rightarrow Ag_2O + H_2O + 2e^-$$

$\varphi^{\ominus}_{O_2/H_2O} = 1.229$ V

$\varphi_{O_2/H_2O}(\text{pH}\sim7) = 0.815$ V

$\varphi^{\ominus}_{Ag_2O/Ag} = 0.342$ V

$\varphi_{Ag_2O/Ag}(\text{pH}\sim7) = 0.756$ V

$$E^{\ominus} = \varphi^{\ominus}_{O_2/H_2O} - \varphi^{\ominus}_{Ag_2O/Ag} = 0.887 \text{ V}$$

$$E = \varphi_{O_2/H_2O}(\text{pH}\sim7) - \varphi_{Ag_2O/Ag}(\text{pH}\sim7) = 0.059 \text{ V}$$

Fig. S3. Proposed redox reactions at silver electrodes during discharge and the analysis of voltage loss introduced by redox reactions. For cells with silver electrodes, the directional ion migration of cations is converted to electron transportation via redox reactions at electrode surface, introducing a voltage loss that could be estimated with the guide of Nernst equation. For GO side, oxygen from the environment might be reduced to water in an acidic environment during discharge process. The theoretical standard electrode potential is 1.299 V (vs. the standard hydrogen electrode, SHE). According to Nernst equation, this potential might decrease to 0.815 V with increasing of pH to 7. For rGO side, silver might be oxidized to silver oxide under alkaline condition. The standard electrode potential is 0.342 V (vs. SHE), and would increase to 0.756 V with decreasing pH to 7. Therefore, the theoretical standard potential for the total reaction is 0.887 V, which would decrease to 0.059 V at neutral condition. In reality, the cell is operating as an all-solid-state power source at various relative humidity without liquid electrolyte, resulting the reaction potential deviate from theory, and the overpotential during discharge process could also affect the reaction potential. Thus, the observed OCV difference between cells with gold current collectors and silver electrodes varies at different relative humidity.

Fig. S4. OCV measurement of a drop-casted sample in Ar-filled glove box (RH ~0%).
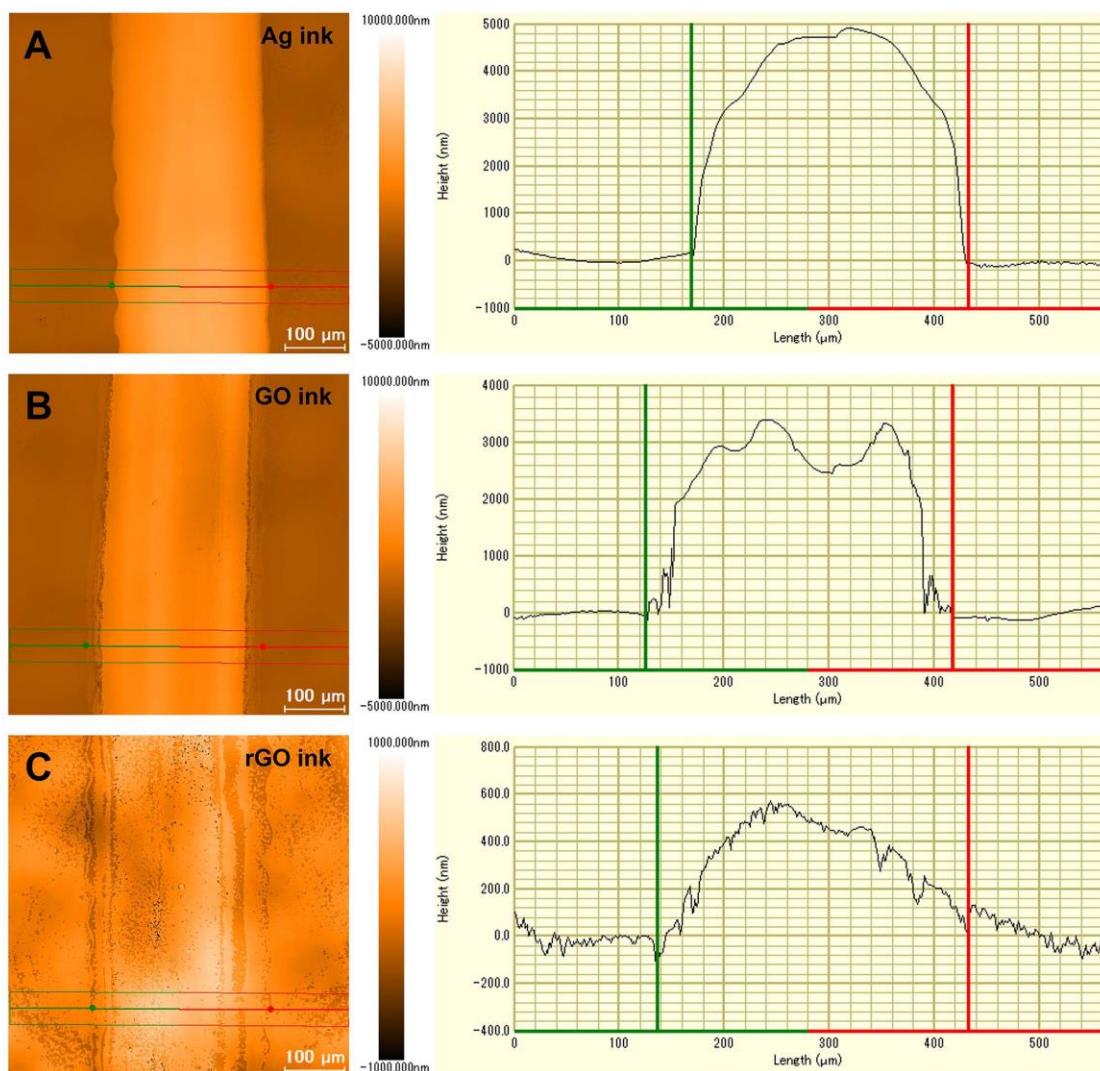
Fig. S5. Height profile measurement by white light interferometric microscope. (*A*) The profile of a strip printed from silver ink. (*B*) The profile of a 10-layer strip printed from GO ink. (*C*) The profile of a 10-layer strip printed from rGO ink.
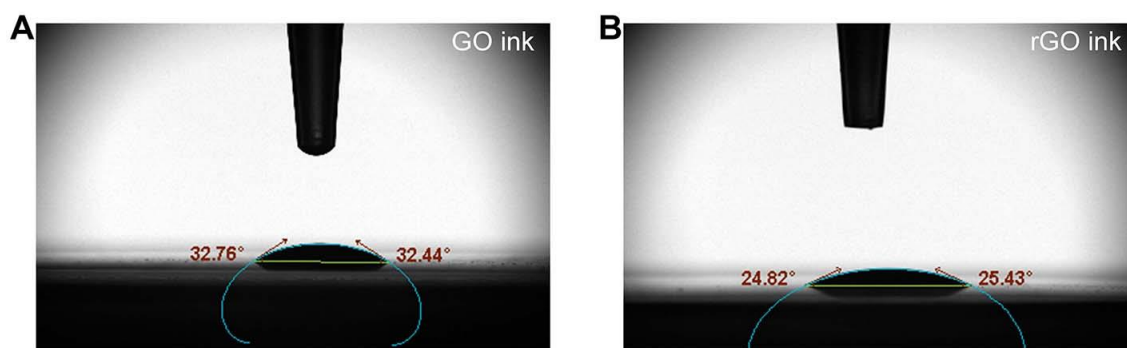
Fig. S6. Contact angle measurement of GO and rGO inks on photo paper substrate. (*A*) The contact angle of GO ink with paper is 32.6°. (*B*) The contact angle of rGO ink with paper is 25.1°.
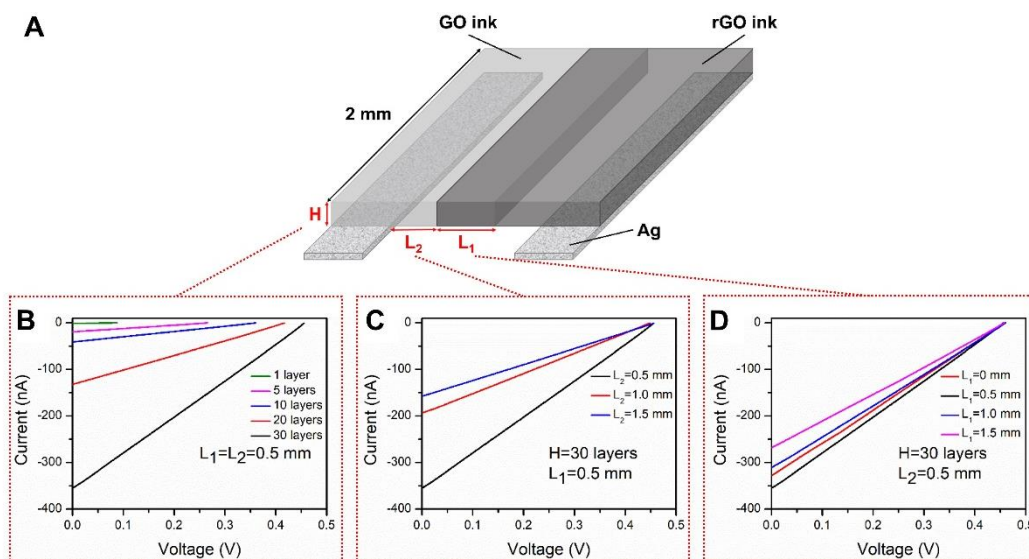
Fig. S7. Schematic of inkjet-printed cell structures and design parameter optimization. (*A*) The schematic structure of a printed cell. (*B*)(*C*)(*D*) The I-V characteristics of cells with different thickness (H), distance to electrodes (L_2) and overlap width (L_1) at 25 °C RH 70%.

Parameter Optimization Analysis. The thickness of a cell (H) is controlled by the repeating times of printing. As shown by I-V characteristics in Fig. S7*B*, with the increasing of H from 1 layer to 30 layers, the OCV increased from 0.086 V to 0.455 V, the short circuit current (I_{sc}) increased from 0.001 µA to 0.355 µA. The reason is that with the increasing thickness, more water could be trapped between the layered structures and more nanofluidic channels are formed to allow the migration of ions. The increase in I_{sc} could be attributed to the lower charge transfer resistance and the raise of OCV is the result of more cations participation in the diffusion process. It should be noted that the OCV will not increase infinitely with the raising thickness, since the number of cations is limited by KOH concentration and hydration degree. The OCV of printed samples might further increase to 0.58 V (OCV of drop-casted samples) with the increasing printing thickness, however, due to the limit of our printing facility and experiment time, we chose 30 layers as our optimized thickness, making the total thickness of printed cell 13 µm. Higher thickness could be easily achieved in the industrial inkjet printer for large scale production.

The distance of printed inks to electrodes (L_2) is an important parameter for the output performance, as shown in Fig. S7*C*. With the decrease of L_2 from 1.5 mm to 0.5 mm, the I_{sc} increased from 0.158 µA to 0.355 µA and the OCV remains about 0.45 V. The increase in I_{sc} is because the distance of cation transportation from rGO to GO is reduced with decreasing L_2. The OCV did not change much since the concentration of cation remains the same. Considering the printing resolution limitation in the laboratory and to prevent short circuit, we chose 0.5 mm as optimized L_2.

The overlap width of GO and rGO inks (L_1) can also influence the output performance (Fig. S7*D*). This overlap is designed to ensure the contact of GO and rGO, while the existence of L_2 prevent the short circuit. With the decrease of L_1 from 1.5 mm to 0 mm, the OCV remains about 0.45 V since there is no cation concentration change. The I_{sc} first increased from 0.268 µA (L_1=1.5 mm) to 0.355 µA (L_1=0.5 mm) and then decreased to 0.328 µA (L_1=0 mm). With the decrease of L_1, the distance between the two electrodes was reduced since L_2 was kept the same. The reduction of average distance of cations transportation from rGO to GO would lower the cell resistance, thus increasing the current. However, when the overlap is too small (L_1=0 mm), the poor contact of GO and rGO will increase the charge transfer resistance and reduce the I_{sc}. Therefore, 0.5 mm was chosen as the optimized overlap width.
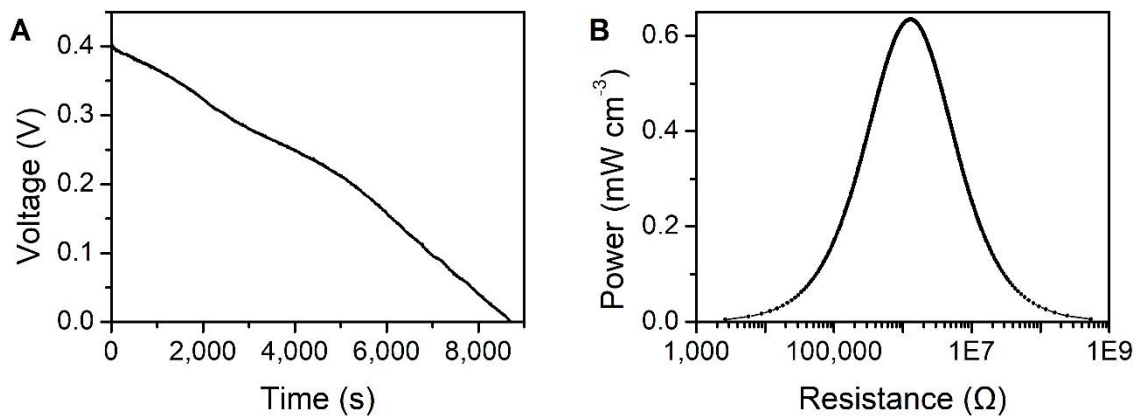
Fig. S8. The output performance of the printed cell (0.2 cm*0.25 cm*13 μm) at 25 °C RH 70%. (*A*) The galvanostatic discharge performance at 0.05 μA and the energy density is calculated to be 0.41 mWh cm^{-3}. (*B*) The power density is calculated from I-V characteristics and the maximum power density is 0.6 mW cm^{-3}.
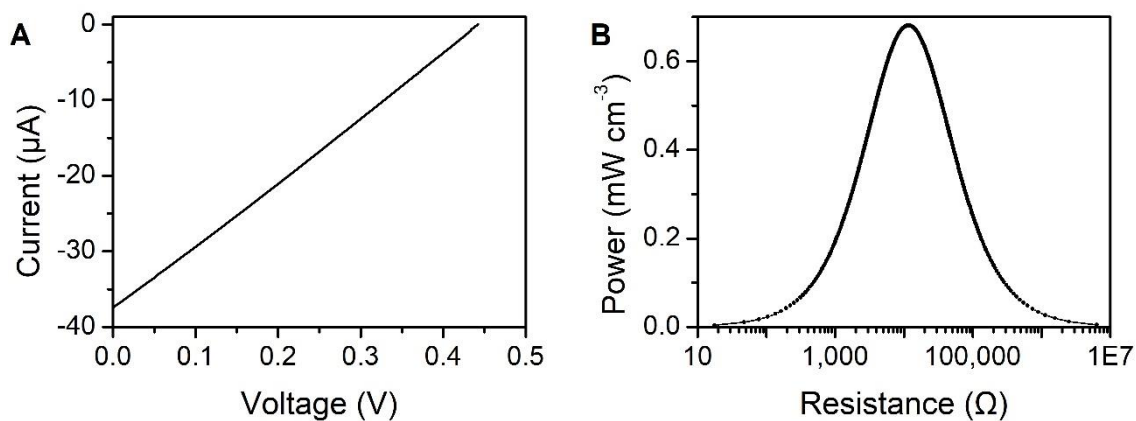
Fig. S9. The output performance of a printed cell with Peano curve pattern at 25 °C RH 70%. (*A*) The I-V characteristics of a printed cell with Peano curve pattern. (*B*) The power density calculated from I-V characteristics.

Movie S1 (separate file). Demonstration of inkjet printing process.

Movie S2 (separate file). Demonstration of the flexibility of the printed cell with ultra-high voltage.